Journal of Environmental Management 240 (2019) 75–83

Contents lists available at ScienceDirect

Journal of Environmental Management

journal homepage: www.elsevier.com/locate/jenvman

Research article

Determining the impacts of climate change and urban expansion on terrestrial net primary production in China

Youyue Wen[a,b], Xiaoping Liu[a,*], Yang Bai[c], Yu Sun[d], Jian Yang[b], Kui Lin[b], Fengsong Pei[e], Yuchao Yan[a]

[a] School of Geography and Planning, Sun Yat-sen University, NO.135 West Xingang RD., Guangzhou, 510275, PR China
[b] South China Institute of Environmental Science, Ministry of Ecology and Environment, NO.18 Ruihe RD., Guangzhou, 510535, PR China
[c] Chinese Research Academy of Environmental Sciences, No.8, Dayangfang, Anwai, Chaoyang District, Beijing, 100012, PR China
[d] Information Center of Ministry of Ecology and Environment, No.1, Yuhui South RD., Chaoyang District, Beijing, 100029, PR China
[e] School of Geography, Geomatics and Planning, Jiangsu Normal University, NO.101 Shanghai RD., Tongshan New District, Xuzhou, 221116, PR China

ARTICLE INFO

Keywords:
Climate change
Urban expansion
Terrestrial net primary production
Relative contributions
China
CASA model

ABSTRACT

Climate change and urbanization strongly affect the variations of terrestrial net primary production (NPP), but the relative contributions of these two factors to NPP changes have not been determined yet (especially on a macroscale). In this study, spatial-temporal variations of NPP in China from 2000 to 2010 were estimated using the Carnegie – Ames – Stanford Approach model, and the effects induced by urbanization and climate change were quantified. The obtained results showed that during the study period, the NPP in China exhibited an annual increase of 0.03 Pg C accompanied by large spatial heterogeneities. During the whole study period, the urban area in China increased by 16.44×10^3 km^2, and the corresponding NPP losses amounted to 11.60×10^{-3} Pg C. Urban expansion significantly offset the climate change-induced NPP increases and worsened NPP decreases (the offsetting ratio calculated for China was 5.42%, and its exact magnitudes varied by province). The largest NPP variations were observed over the regions with rapid urban expansion, whose contribution ratio was 32.20% for China and exceeded 30% for most provinces. Climate change contributed considerably to the NPP variations in both the newly urbanized (30.45%) and purely vegetated (46.92%) areas, but its contribution ratios were slightly lower than those of residual factors. Moreover, climate change strongly affected the NPP levels over the arid and semi-arid regions as well as over the Tibet Plateau; however, residual factors dominated the NPP variations over the central and southeast China. Our study highlights a significant role of urbanization in driving terrestrial NPP variations on a macroscale and provides a new perspective on disentangling the impacts of external factors on NPP values.

1. Introduction

Terrestrial net primary production (NPP) is the net amount of organic biomass accumulated by plants per unit area and time (Potter et al., 1993; Roxburgh et al., 2005). As a key component of the global carbon cycle, NPP reflects the production capacity of vegetation in the natural environment and provides fundamental sources of materials, food, and fuel for human activities and life (Krausmann et al., 2013; Yu and Chen, 2016). Variations in NPP reflect changes in the structure and operation of the terrestrial ecosystem and affect its development (Nemani et al., 2003; Potter et al., 2012; Zhao and Running, 2010). Hence, studying the spatio-temporal dynamics of terrestrial NPP and its interactions with external driving forces is of critical importance (Gu et al., 2017; Potter et al., 2012; Wu et al., 2014; Zhao and Running, 2010).

Climate change and land use/cover change (LUCC) are two of the most important driving forces for NPP variations (Wu et al., 2014; Yan et al., 2018b), which result in fluctuations of the photosynthetic and respiration rates, water use efficiency, and nutrition availability of green plants and strongly affect the structure and operation of terrestrial ecosystems (Sun et al., 2018; Thomas et al., 2016; Yan et al., 2016). While high inconsistences exhibited among different studies. For example, some researchers reported a global increase in the NPP level from 2000 to 2009 (Potter et al., 2012), while others observed decreasing NPP trends on the global scale (Zhao and Running, 2010). These discrepancies can be related to various natural and human-made phenomena, such as increasing climatic fluctuations and fine-scale LUCC (Liu et al., 2017; Potter et al., 2012). Therefore, additional studies

* Corresponding author.
E-mail address: liuxp3@mail.sysu.edu.cn (X. Liu).

https://doi.org/10.1016/j.jenvman.2019.03.071
Received 11 July 2018; Received in revised form 15 March 2019; Accepted 15 March 2019
Available online 28 March 2019
0301-4797/ © 2019 Elsevier Ltd. All rights reserved.

must be performed to elucidate the effects of climate change and LUCC on NPP.

As the most dramatic type of LUCC, urban expansion strongly influences NPP variations and serves as one of the most critical disturbance factors affecting the carbon cycle (Imhoff et al., 2004; Tian and Qiao, 2014; Wu et al., 2014). On the one hand, urbanization can significantly decrease the terrestrial NPP (Imhoff et al., 2004; Pei et al., 2013b), which is often accompanied by the direct degradation of highly productive vegetation ecosystems as well as by indirect adverse effects such as the reduced functionalities of ecosystems and human energy demands (Imhoff et al., 2004; Jiang et al., 2015; Song and Deng, 2015). On the other hand, urban expansion can also increase the terrestrial NPP value under certain circumstances, including various activities associated with sea reclamation engineering and anthropogenic management (Pei et al., 2013b; Zhang et al., 2014a). The effect of urban expansion on NPP is very diverse; however, it has not been examined in detail yet (especially on a microscale) due to the existing land cover defects such as the coarse spatial resolution and limited time span (Chen et al., 2015; Jiang et al., 2015; Pei et al., 2013b).

Generally, factors affecting the terrestrial NPP are analyzed with either statistical or scenario simulation methods (Song and Ma, 2011; Xiao et al., 2015; Yan et al., 2018a). The former approach is relatively simple; however, it possesses a limited ability to express results in a spatially explicit way (Song and Ma, 2011; Xiao et al., 2015). In contrast, scenario simulation methods utilizing process-based models can remedy this defect and are often used as controllable and effective techniques for distinguishing the effects of different factors on NPP variations (Wu et al., 2014; Yan et al., 2016; Zhang et al., 2014b). However, due to the complexity of the impacts of climate change and urban expansion on NPP coupled with the absence of a suitable assessment methodology, the recent studies involving scenario simulation methods have made very little progress in disentangling these two factors, and their relative contributions remain poorly understood (especially on a macroscale) (Pei et al., 2015; Wu et al., 2014).

China, the third largest country in the world, is a good candidate for studying the interactions between environmental changes and the carbon cycle. In recent decades, China has been experiencing a dramatic climate change as well as intense urbanization on a large scale (Gu et al., 2017; Liu et al., 2012a; Yan et al., 2016). An increasingly large number of studies have documented the highly complex impacts of climate change and urbanization on the NPP variations in China (Gu et al., 2017; Jiang et al., 2015; Pei et al., 2015; Xu et al., 2014). However, these studies either used low spatial resolution land cover data or were conducted on a small scale and thus did not properly quantify the contributions of climate change and urbanization to NPP variations. Therefore, the objectives of this work were to (1) analyze the spatial-temporal changes in NPP observed in China from 2000 to 2010, (2) disentangle the impacts of climate change and urban expansion on the NPP level over the study area, and (3) assess the relative contributions of different factors on NPP variations on the national scale. For this purpose, we first evaluated the terrestrial NPP in China from 2000 to 2010 by using the Carnegie-Ames-Stanford Approach (CASA) model. Next, the NPP variations induced by climate change, urban expansion, and residual factors were separated based on the scenario simulation concept. Finally, a contribution separating method was utilized to determine the relative contributions of these factors to NPP variations.

2. Methods

The datasets used in this study were summarized in Supplementary Material (Table S1) (Didan, 2015; FAO et al., 2012; Friedl and Sulla-Menashe, 2015; Harris et al., 2014; Sheffield et al., 2006). The study period spanned over the first decade of the 21st century (2000–2010), during which China has undergone unprecedented urbanization caused by globalization at a growth ratio that was about 2.5 times greater than the magnitude observed in the late 20th century (Yan et al., 2016). In addition, although various datasets are now available for the recent years, there are only two years' data (2000 and 2010) of the urban coverages obtained from the National Geomatics Center of China (GlobeLand30) (Chen et al., 2015). To ensure the consistency of the input datasets, their temporal spans were unified.

2.1. CASA model for NPP estimation

The CASA model is a light-use efficiency (LUE) technique that was originally proposed by Potter et al. (1993). It utilizes easy-to-obtain parameters including the normalized difference vegetation index (NDVI) and monthly average air temperature (TEM), monthly total precipitation (PRCP), and monthly downward short-wave solar radiation (SOLAR) as well as vegetation maps and soil properties (Potter et al., 1993). In this model, the NPP was estimated via the following formula:

$$\mathrm{NPP} = 0.5 \times \mathrm{SOLAR} \times \mathrm{FPAR} \times T_1 \times T_2 \times W_s \times \varepsilon_{max} \quad (1)$$

where the factor 0.5 represents the fraction of the active incoming solar radiation used by vegetation; FPAR is the fraction of the photosynthetically active radiation absorbed by vegetation, which is a function of NDVI; T_1 denotes the effects of the extremely low and high temperatures on LUE; T_2 reflects the situation when the temperature is either above or below the optimum temperature (∘C) and when the NDVI reaches its maximum value throughout the year (both T_1 and T_2 depend on TEM and the optimum temperature); W_s represents the moisture effect on the vegetation growth and is a function of TEM and PRCP; and ε_{max} (g C·MJ^{-1}) is the maximum LUE determined for plants under the optimal living conditions. The detailed calculation steps for each parameter were documented by Potter et al. (1993).

ε_{max} is an important attribute of plants and a key parameter of the CASA model (Potter et al., 1993; Zhu et al., 2006), whose value depends on the spatial scale and vegetation type (Pei et al., 2013b; Yan et al., 2018b; Zhu et al., 2006). In this study, the CASA model was calibrated by computing a set of ε_{max} values for different vegetation types using the algorithm of modified least squares. This method was originally proposed by Zhu et al. (2006) and has been successfully utilized in previous studies (Pei et al., 2013b; Wen et al., 2018; Zhu et al., 2007).

2.2. A neighborhood proxy method for calculating the pre-urban NPP

Multiple land cover types, such as trees, lawns, and impervious surfaces, are present in an urban landscape; as a result, it is extremely difficult to directly estimate the LUE and related NPP values for urbanized areas (Imhoff et al., 2004; Pei et al., 2013b). In this study, a neighborhood proxy method was used to determine the urban NPP in a pre-urban situation (pre-urban NPP), which was defined as the condition of natural vegetation distribution without any urban land development. This method was based on the assumption that non-urban land surfaces were the best proxy for nearby urban land before they were transformed (Imhoff et al., 2004; Li et al., 2016b; Pei et al., 2013b). The pre-urban NPP for an urban cell was computed by replacing the current NPP (post-urban NPP) value with the mean post-urban NPP magnitude computed for the adjacent non-urban cells containing the original vegetation types (see Fig. 1). This procedure was performed for the area with a 100-km radius in each urban cell to cover all big cities in China (Imhoff et al., 2004; Pei et al., 2013b).

2.3. Scenario simulation design

Three different scenarios, including the real situation, climate-driven, and urbanization-driven ones, were considered to assess the NPP changes induced by external factors (Table S2) (Li et al., 2016a; Wu et al., 2014, 2017). In the real situation scenario, the terrestrial NPP was predicted from the input data available for the 2000–2010 period

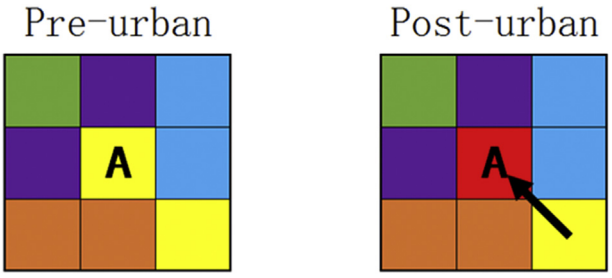

Fig. 1. A schematic diagram of the neighborhood proxy method. If an urbanized pixel "A" was originated from a crop land pixel (yellow grid), we replaced the current NPP of "A" (post-urban NPP) with the nearby mean post-urban NPP of crop land pixels. (For interpretation of the references to color in this figure legend, the reader is referred to the Web version of this article.)

(Table S2). Note that FPAR, a function of NDVI, is a comprehensive factor that takes into account the effects of climate change (Nemani et al., 2003; Pei et al., 2015), LUCC (Li et al., 2017; Liu et al., 2017), CO_2 fertilization (Thomas et al., 2016) and N deposition (Finzi et al., 2007). Thus, the residual factors (the non-climatic and non-urbanization ones) were simulated in the real situation scenario by considering FPAR variations in the CASA model. In the climate-driven scenario, it was assumed that NPP variations were influenced only by climate change, and climatic factors were allowed to change, while the FPAR and land cover were set to constant values obtained for 2000 to eliminate the disturbing effects on NPP variations induced by non-climatic factors (Table S2) (Wu et al., 2014; Yan et al., 2016; Zhang et al., 2014b). For the urbanization-driven scenario, we assumed that NPP variations were affected only by urban expansion and used the changing urban extent (GlobeLand30) and constant external conditions to estimate NPP values (Table S2) (Imhoff et al., 2004; Wu et al., 2014). It was also hypothesized that no or little changes in LUCC occurred in a single year, and the same land cover and urban extent data were used for the monthly driven CASA model. The urban extent for each year between 2000 and 2010 was calculated using the parameters extracted from the GlobeLand30 database, assuming a constant expansion speed. The pre-urban NPP in the newly urbanized area over the studied period was estimated through the neighborhood proxy method. The NPP losses for the same area caused by the urban expansion in 2000–2010 were calculated as the negative pre-urban NPP level by treating the urban land as a carbon source (i.e. assuming that the post-urban NPP was zero) (Imhoff et al., 2004; Pei et al., 2013b; Wu et al., 2014).

2.4. Calculation of the impacts of external factors on NPP variation

The factors affecting NPP variations were classified into climatic, urbanization, and residual ones. The temporal trends of the real situation and climate-driven NPP were spatially computed using a linear regression method (Wu et al., 2014; Zhang et al., 2007). The resulting slopes represented the contributions of the climate change (ΔNPP_{Clm}) and all external factors (ΔNPP_{All}) to NPP variations.

$$\text{Slope} = \frac{n \times (\sum_{i=1}^{i=n} X_i \times Y_i) - (\sum_{i=1}^{i=n} X_i) \times (\sum_{i=1}^{i=n} Y_i)}{n \times (\sum_{i=1}^{i=n} X_i^2) - (\sum_{i=1}^{i=n} X_i)^2} \quad (2)$$

where n is the total number of years, X_i represents the year series from 2000 to 2010, and Y_i represents the annual NPP from 2000 to 2010.

The NPP changes in the urbanization-driven scenario (ΔNPP_{Urb}) were calculated as the slope of the urbanization-driven NPP amount plotted as a function of time assuming a fixed rate of the urban sprawl during the 2000–2010 period (Equation (3)). The trend for the residual factor-driven scenario (ΔNPP_{Res}, Equation (4)) was determined as the difference between the real situation NPP changes (ΔNPP_{All}) and the sum of the climate-driven (ΔNPP_{Clm}) and urbanization-driven (ΔNPP_{Urb}) NPP changes (Wu et al., 2014).

$$\Delta NPP_{Urb} = \frac{NPP_{pre_Urb} - NPP_{post_Urb}}{10} \quad (3)$$

$$\Delta NPP_{Res} = \Delta NPP_{All} - \Delta NPP_{Clm} - \Delta NPP_{Urb} \quad (4)$$

where NPP_{pre_Urb} is the pre-urban NPP and NPP_{post_Urb} is the post urban NPP.

2.5. Calculation of the relative contributions of external factors to NPP variation

As shown in Equation (5) – (7), the contribution ratios of climate change (Ctr. Clm), urban expansion (Ctr. Urb), and residual factors (Ctr. Res) were alternately determined as the proportions between the absolute values of the climate-driven NPP, urbanization-driven NPP, residual factor-driven NPP, and their sum (Wu et al., 2014).

$$Ctr.Clm = \frac{|\Delta NPP_{Clm}|}{|\Delta NPP_{Clm}| + |\Delta NPP_{Urb}| + |\Delta NPP_{Res}|} \times 100\% \quad (5)$$

$$Ctr.Urb = \frac{|\Delta NPP_{Urb}|}{|\Delta NPP_{Clm}| + |\Delta NPP_{Urb}| + |\Delta NPP_{Res}|} \times 100\% \quad (6)$$

$$Ctr.Res = \frac{|\Delta NPP_{Res}|}{|\Delta NPP_{Clm}| + |\Delta NPP_{Urb}| + |\Delta NPP_{Res}|} \times 100\% \quad (7)$$

where $|\Delta NPP_{Clm}|$ and $|\Delta NPP_{City}|$ denote the impacts of climate changes and urban expansion on NPP, respectively, and $|\Delta NPP_{Res}|$ represents the impact on NPP that was unexplained by both urban expansion and climate changes.

3. Results

3.1. Validation of predicted NPP

To verify the reliability of the utilized CASA model, the predicted NPP values were compared with the annual NPP determined by the MODIS land algorithm (MOD17A3) and CASA model developed by Pei et al. (2013a) (Figs. S1eS2). By performing comparisons for the randomly distributed points across China (Fig. S1), high correlation coefficients were obtained for the NPP values determined in this work and those computed using the MOD17A3 algorithm (0.76 for the *Natural Tall Vegetation*, 0.87 for the *Natural Short Vegetation*, 0.72 for the *Developed and Mosaic Lands*, and 0.80 for all vegetation types; see Fig. S1a). Similarly, high correlation coefficients were obtained for the NPP values computed in this study and by Pei et al. (2013a) (0.72 for the *Natural Tall Vegetation*, 0.92 for the *Natural Short Vegetation*, 0.79 for the *Developed and Mosaic Lands*, and 0.86 for all vegetation types; see Fig. S1b). The average NPP values calculated for different vegetation types (Fig. S2) in this work matched very well with the MOD17A3 data (R = 0.96; Fig. S2a) and the results obtained by Pei et al. (2013a) (R = 0.99; Fig. S2b). In addition, the average annual NPP in China estimated for the period from 2000 to 2010 was 2.36 Pg C (ranging from 2.14 Pg C to 2.57 Pg C), which was within the reported interval of 1.43–4.60 Pg C (Table S3) (Feng et al., 2007; Gao et al., 2012; Gao and Liu, 2008b; Gu et al., 2012; Liu et al., 2012b; Pei et al., 2013a; Wang et al., 2017; Wang, 2004). Moreover, the annual NPP trend obtained from 2001 to 2010 was very similar to that determined by Pei et al. (2013a) (Fig. S3).

3.2. Spatial-temporal distributions and variations of NPP trend

In the real situation scenario (Fig. 2a), the NPP in China exhibited a generally increasing trend from 2000 to 2010, which was accompanied by large spatial heterogeneities. This trend was extremely strong over the south and central regions of China, Northeast China Plain, North China Plain, and Loess Plateau. However, strong negative NPP trends were also observed for other regions, including the eastern Tibet and

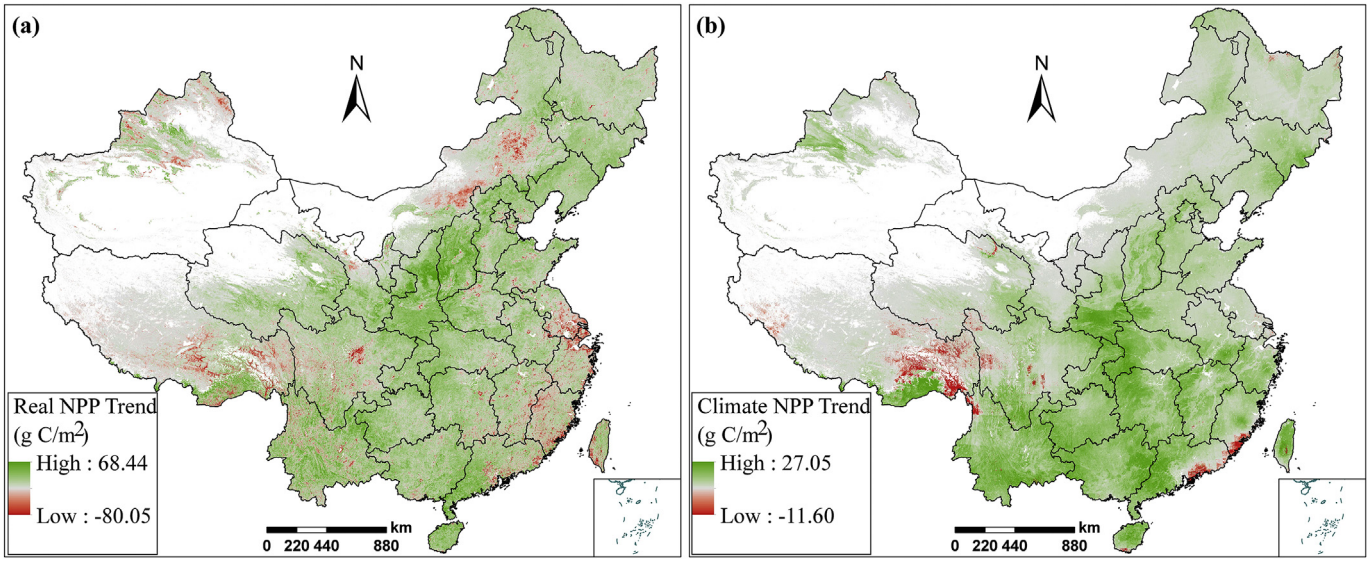

Fig. 2. Spatial distributions of real-situation (a) and climate-driven (b) NPP trends in China from 2000 to 2010. These maps were produced by computing the linear trends at a pixel level based on the annual NPP during the 10-year interval period.

south China, central and eastern parts of the Inner Mongolia, and urbanized and metropolitan areas in China. The NPP magnitudes determined for the climate-driven scenario demonstrated large spatial heterogeneities across the entire country with relatively large values calculated for its middle and south parts, and smaller values computed for other regions (Fig. 2b). These patterns were very similar to that obtained for the real situation scenario. The negative NPP trends observed in the climate-driven scenario were less apparent than that obtained in the real situation scenario and demonstrated extremely high values for the eastern Tibet, Guangdong Province, and Fujian Province.

The average annual NPP in China determined for the period from 2000 to 2010 in both the real situation and climate-driven scenarios was 2.36 Pg C, and the slopes of the corresponding linear plots (Fig. 3) were 0.03 Pg C/year (R = 0.77) and 0.02 Pg C/year (R = 0.72), respectively. Thus, the annual NPP exhibited similar variations in these scenarios (its magnitude went up and down interactively from 2000 to 2005, after which it increased sharply until 2008 and then gradually decreased until 2010).

3.3. Urban expansion and its impact on NPP variations

3.3.1. Urban expansion area

The urban area in China was 145.26 × 10^3 km^2 in 2000. From 2000 to 2010, it increased by 16.44 × 10^3 km^2, which was equal to 11.32% of the total urban land in 2000. The fractional urban expansion map depicted in Fig. 4a shows that urban expansion largely occurred in East China and the Northeast and North China plains during the 10-year period. In addition, the three coastal urban agglomerations — the Beijing-Tianjin-Hebei, Yangtze River Delta, and Pearl River Delta regions — exhibited very rapid urban expansions. The top 5 provinces

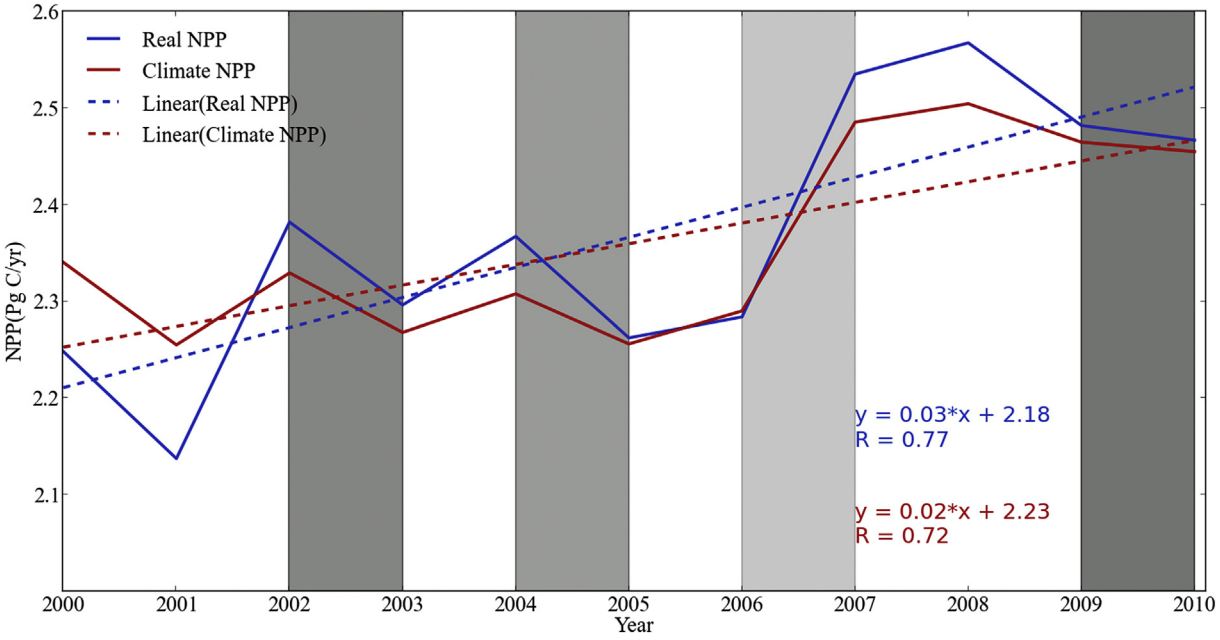

Fig. 3. Inter-annual variations and corresponding linear trends of real-situation (blue line) and climate-driven (red line) NPP in China from 2000 to 2010 at country level. The El Niño years were shown in gray bars, where darker bars represent stronger El Niño event. (For interpretation of the references to color in this figure legend, the reader is referred to the Web version of this article.)

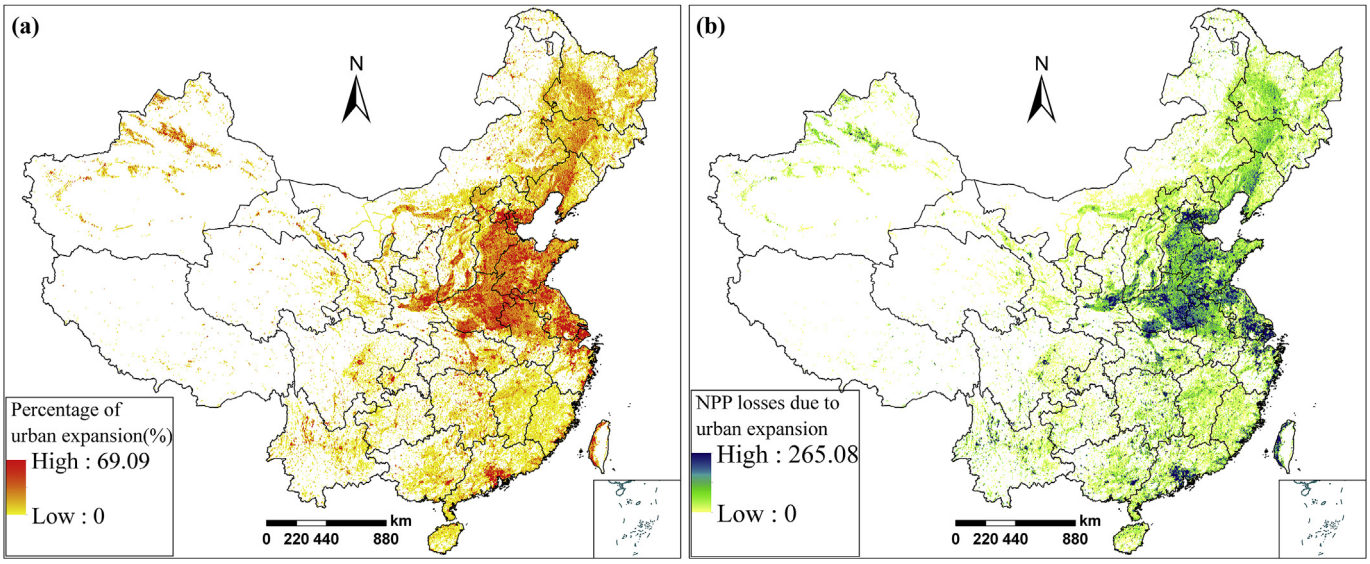

Fig. 4. Spatial distributions of the fractional urban expansion in China (a) and related NPP losses (b) observed over the period from 2000 to 2010. Panel (a) was produced by subtracting the GlobeLand30 data obtained in 2010 from those obtained in 2000. Panel (b) was produced by multiplying the data shown in Fig. 4a by the NPP values obtained in the urbanization-driven scenario.

with the largest urban expanded areas of 2.36, 2.24, 1.25, 1.15, and 1.05 × 10^3 km^2 (which corresponded to a nearly half (49.00%) of the total urban expansion area in the entire country) were Jiangsu, Shandong, Hebei, Anhui, and Zhejiang (Table S4). The highest urban growth rates were observed for the four municipalities of Tianjin (45.00%), Chongqing (44.87%), Shanghai (39.22%), and Beijing (37.77%).

3.3.2. NPP losses caused by urban expansion

The NPP losses caused by the urban expansion in China during the 2000–2010 period were equal to 11.60 × 10^{-3} Pg C. The results presented in Fig. 3b indicate that NPP losses were widely distributed across East China and the Northeast and North China plains and were most serious in the regions with strong urban expansion (such as the Beijing – Tianjin – Hebei, Yangtze River Delta, and Pearl River Delta ones) demonstrating high levels of carbon emissions over these ecosystems. The highest NPP losses were observed for the Henan (1.30 × 10^{-3} Pg C), Shandong (1.24 × 10^{-3} Pg C), Jiangsu (1.02 × 10^{-3} Pg C), Anhui (0.79 × 10^{-3} Pg C) and Hebei (0.79 × 10^{-3} Pg C) provinces, which accounted for 44.23% of the total NPP loss over the entire country (Table S4). By comparing the top 5 provinces with the largest urban expansion areas to those with the highest urbanization-induced NPP losses (Table S4), it can be seen that Zhejiang is not included into the second category, and that the average NPP values determined for the newly urbanized areas of these provinces are not the same. For example, although the total urban expansion area of the Jiangsu province was larger than that of the Shandong province, the average NPP magnitude obtained for the newly urbanized areas of the latter (272.22 g C/m^2) was greater than that of the former (232.90 g C/m^2). Similar phenomena have been observed for other provinces, such as Zhejiang and Anhui, indicating that although the urban expansion area plays a major role in determining the urbanization-induced NPP losses, the average NPP in the newly urbanized areas is another important factor that cannot be ignored.

A comparison of the NPP trends obtained for the climate-driven and urbanization-driven scenarios (Table S4) shows that urban expansion tends greatly offset the NPP increases caused by climate change. The offsetting ratio calculated for China was 5.42%, and its exact magnitudes varied by province. The offsetting ratios determined for Jiangsu (219.00%) and Shanghai (129.61%) exceeded 100%; the values computed for Tianjin (68.90%) and Shandong (53.48%) exceeded 50%; and the offsetting ratios calculated for Henan (38.95%), Macao (36.48%), Beijing (30.51%), and Anhui (29.04%) exceeded 20% (lower values were obtained for other provinces). Hong Kong was an exception: its urban expansion worsened the negative NPP trend caused by climate change (269.74%).

3.4. Relative contributions of urbanization and climate change to NPP variations

Among the newly urbanized areas, the contributions of urban expansion (Fig. 5a) were extremely high in the three coastal agglomerations and other metropolitan regions in China (including Zhengzhou, Nanjing, Hefei, and Chengdu). The nationwide contribution ratio of urban expansion was 32.20%, and its magnitude exceeded 30% in most provinces (Table S4). The highest value was obtained for Hong Kong (55.23%), and the lowest one – for Ningxia (21.73%). Climate change also affected the NPP variations in the newly urbanized areas, and its overall contribution ratio was 30.45% (Table S4). Generally, the climate change-driven contribution ratio exhibited a spatially decreasing trend from the south to the north (Figs. 5b and d), and its highest values were obtained for Jiangxi (56.83%) and Guizhou (53.75%), and the lowest ones – for Hong Kong, Shanghai, and Ningxia (less than 15%). By comparison, the nationwide contribution ratio of residual factors in the newly urbanized areas was higher than that of climatic factors (37.35%). The residual factors-driven contribution ratio exhibited an opposite spatial distribution trend as compared to that obtained for the climate change-driven contribution ratio (Figs. 5c and d); it reached the highest values in Ningxia, Gansu, Qinghai, and Liaoning (above 50%) and the lowest ones – in Jiangxi and Guizhou (below 15%).

In the purely vegetated areas, the climate change-driven contribution ratio calculated for the NPP change over the entire country was 46.92% (Table S4), which was slightly lower than that determined for residual factors (53.08%). The climate change-driven contribution to the NPP change exhibited a generally increasing spatial trend from the southeast coast to the northwest inland with extremely high values obtained for the arid and semi-arid regions (Fig. 5b and d), as opposed to the trend observed for residual factors (Fig. 5c – d). The provinces in Northern China, such as Ningxia (80.79%), Qinghai (70.59%), Gansu (68.72%), Shanxi (63.32%), and Inner Mongolia (60.76%) had very high contribution ratios due to climate change (above 60%). At the same time, the provinces in Southern China including Hunan (68.37%), Guangxi (65.86%), Guizhou (64.43%), Jiangxi (63.09%), Taiwan

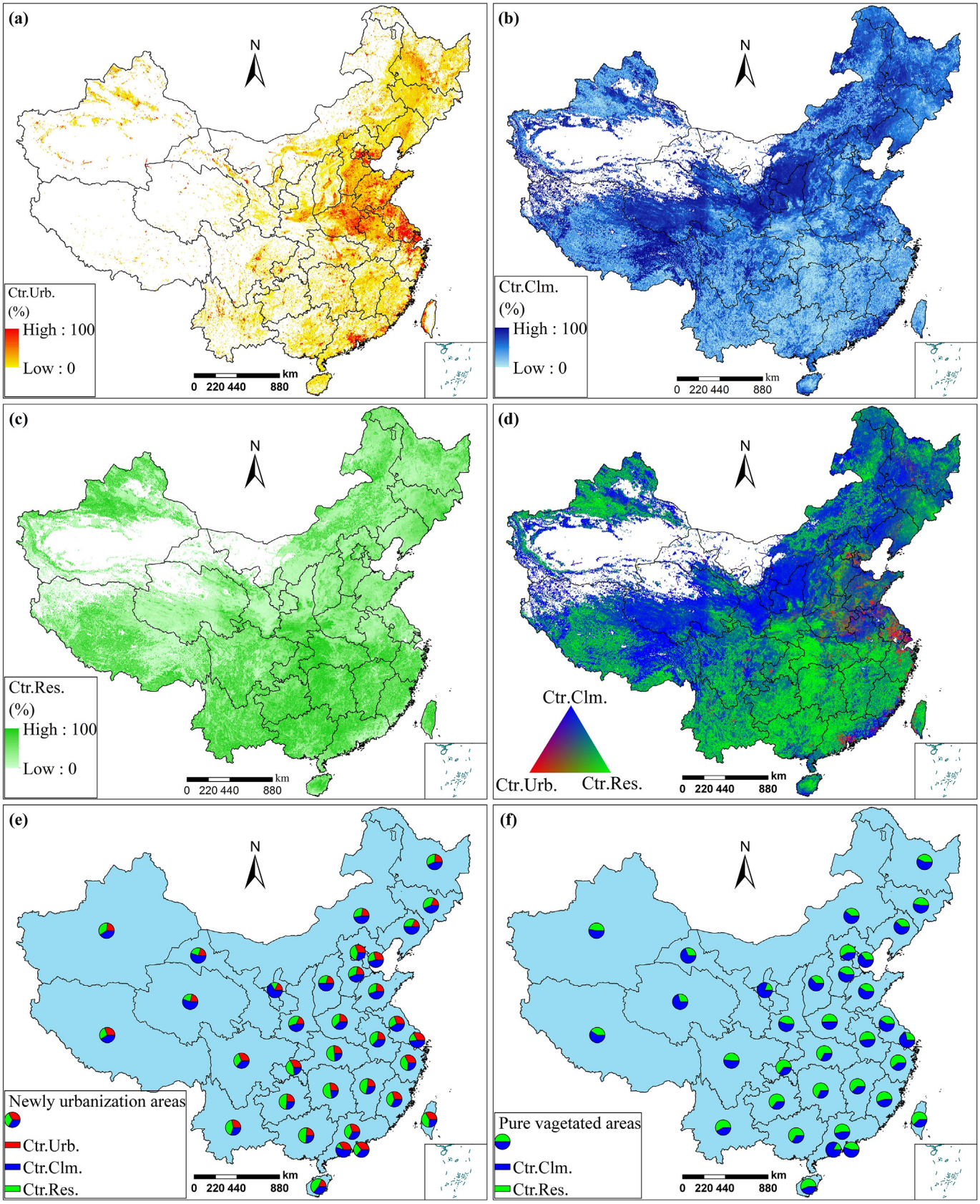

Fig. 5. Spatial distributions of the contribution ratios of urbanization (a), climate change (b), and residual factors (c) determined for the variations in the terrestrial NPP level from 2000 to 2010. A composite map constructed for panels (a), (b), and (c) using a Maxwell color triangle to visualize the relative contributions of each factor to NPP variations (d). Relative contributions of the three external factors to the NPP variations in the newly urbanized (e) and purely vegetated (f) areas determined for different provinces. (For interpretation of the references to color in this figure legend, the reader is referred to the Web version of this article.)

(61.48%), and Zhejiang (61.06%) exhibited very high contribution ratios due to residual factors (above 60%).

4. Discussion

4.1. Evaluation of the NPP results

Previously, Gao et al. (2012) determined that the annual NPP in China varied between 1.43 and 4.60 Pg C after comparing 36 estimates obtained by different models for the 1980–2000 period. Liu et al. (2012b) found that during 2001–2010, the annual NPP level determined by a process-based boreal ecosystem productivity simulator model was in the range of 2.63–2.84 Pg C. Pei et al. (2013b) reported that the annual NPP in China estimated by the CASA model varied from 2.25 to 2.63 Pg C (average value: 2.54 Pg C) during the same period. The annual NPP level in China during 2000–2010 estimated in this study (varied from 2.14 to 2.57 Pg C with an average value of 2.36 Pg C) was consistent with these values (Table S3; in particular, with the results obtained by Pei et al. (2013a) because the same model and similar input datasets and study periods were used in both works). From the seasonal variations in the NPP level obtained for different vegetation types (Fig. S4), it was found that the evergreen broadleaf forest in China peaked at August, while the other vegetation peaked at July, which was in good agreement with the results of previous studies (Pei et al., 2013b; Sun and Zhu, 2001). In addition, the average NPP values determined for different vegetation types in this study were compared with the magnitudes computed in other works (Gao et al., 2012; Liang et al., 2015; Liu et al., 2012b; Pei et al., 2013a; Piao et al., 2005; Running et al., 2000; Sun and Zhu, 2001). The obtained results (Table S5) showed that the same vegetation types exhibited different NPP values in various studies, likely due to different models, input datasets and studying periods used in these studies (Gao and Liu, 2008a; Shao et al., 2016). The data presented in this work were comparable with the results obtained by Pei et al. (2013a), the MOD17A3 model, and Gao et al. (2012) with R values greater than 0.95 (Table S5). Moreover, higher uncertainties of NPP estimates were observed for forests than for other biomes in this and other studies (such that of Pei et al. (2013a) and when using the MOD17A3 algorithm (Fig. S1)).

4.2. Spatio-temporal NPP trends

The spatio-temporal NPP trends exhibited very similar patterns for the real situation and climate change-driven scenarios (Fig. 2), suggesting that the growth of vegetation in China was largely associated with climate change (Song and Ma, 2011; Sun and Zhu, 2001; Zhu et al., 2007). However, these trends were also characterized by large spatial heterogeneities in both scenarios, which were likely related to the existence of complex ecological relationships between the vegetation growth and external factors (Gu et al., 2017; Xu et al., 2014). The obtained NPP values varied by province (Table S4), which might be due to the different vegetation growth conditions (Xiao et al., 2015). In the real situation scenario (Fig. 2a), the Loess Plateau exhibited strong increasing NPP trends; however, the central and eastern parts of the Tibetan Plateau and Inner Mongolia demonstrated strong decreasing NPP trends, which were consistent with the results obtained by Ouyang et al. (2016) who also observed degraded services in the former ecosystems and improvement in the later ecosystems' services during 2000–2010.

In general, the El Niño phenomenon had a negative impact on NPP (Nemani et al., 2003). During the 2000–2010 period, the El Niño was observed from 2002 to 2003, from 2004 to 2005, from 2006 to 2007, and from 2009 to 2010. Fig. 3 shows that the annual NPP decreased dramatically during these years except for the 2006–2007 period when the NPP exhibited a strong increasing trend due to the large area of China's territory with the monsoon climate. The monsoon circulation changed the combinations and distributions of various climatic factors, which resulted in a complex relationship between the El Niño events and NPP variations, as was observed by Zhu et al. (2007).

4.3. Effects of external factors on NPP variations

The urbanization in China has led to dramatic carbon flux fluctuations. It was reported that China's terrestrial NPP decreased by 0.95×10^{-3} Pg C during 1989–2000 (Tian and Qiao, 2014) and by 3.1×10^{-3} Pg C during 2000–2006 (Pei et al., 2013b); moreover, the NPP in the Pearl River Delta region decreased by 0.10×10^{-3} Pg C during 2000–2005 and by 0.03×10^{-3} Pg C during 2005–2010 (Jiang et al., 2015). Using the GlobeLand30 dataset with high spatial resolution, we quantified the expansion of the impervious surface in China during 2000–2010 and related NPP losses. Large urban expansions occurred in the three coastal agglomerations, four municipalities, and other major economic provinces (Fig. 4a) (Chen et al., 2015; Li et al., 2017; Liu et al., 2017) and were accompanied by huge NPP losses (Fig. 4b) (Jiang et al., 2015; Wu et al., 2017; Yan et al., 2018b). The contributions of urban expansion to NPP variations (Fig. 5a) were extremely high in these regions, which was in good agreement with the results of previous studies (Tian and Qiao, 2014; Wu et al., 2014).

The positive effects of climate change observed in the Tibetan Plateau (Fig. 2) were attributed to the rising temperature (Fig. S5a), which enhanced the photosynthesis process and lengthened the growing season (Gu et al., 2017; Zhu et al., 2016). At the same time, the increasing NPP trends in South and Central China (Fig. 2) can be related to the high levels of precipitation (Fig. S5b) and solar radiation (Fig. S5c) (Liang et al., 2015; Xu et al., 2014). The negative NPP trends observed in Eastern Tibet, Guangdong Province, and Fujian Province (Fig. 2b) likely resulted from the reduced precipitation (Fig. S5b) and longer droughts during the 2000–2010 period (Li et al., 2016a; Mao et al., 2015). In the arid and semi-arid regions of China, precipitation, rather than temperature and solar radiation, exhibited changing patterns (Fig. S5) similar to those of the NPP trends (Fig. 2b), which suggested that precipitation correlated more strongly with NPP over these regions (Song and Ma, 2011; Wang et al., 2016). The spatial patterns of the NPP variations in the southwestern part of China (Fig. 2b) more closely resembled those of solar radiation than the patterns obtained for precipitation and temperature (Fig. S5), indicating that solar radiation was a major climatic factor affecting the vegetation growth there (Tian et al., 2011; Zhu et al., 2007).

A significant part of the observed NPP variations cannot be explained by climate change or urbanization on both the national and provincial levels (denoted as the residual contributions in this work; see Fig. 5c – f, Table S4). Their magnitudes were extremely high over the southeastern and central parts of China, which was consistent with the results of several previous studies. For example, Zhu et al. (2016) reported that the greening vegetation trends observed from 1982 to 2009 in Southeastern China were dominated by the rising CO_2 level, while the central parts of China were mostly affected by the LUCC and other factors such as forest management, grazing, cultivation practices, and irrigation. Lu et al. (2012) found that the increased N deposition level resulted in a net carbon sink of 62 Tg C/year in China's terrestrial ecosystems, and its largest value was obtained in Southeast China during 1901–2005. Furthermore, Ren et al. (2007) revealed that the elevated tropospheric O_3 level resulted in a mean 4.5% reduction in the NPP of China and 0.9% reduction in the total carbon storage nationwide from 1961 to 2000 (the strongest effect was observed in East-central China). By performing spatial visualization, this study provided an objective perspective on the relative contribution of each factor to NPP variations (Fig. 5). The regions with strong residual contributions can be examined in more detail to determine specific factors affecting NPP changes in future studies.

4.4. Uncertainties

This study highlights a significant role of urbanization in driving

NPP changes on a macroscale and provides a new perspective on disentangling the effects of external factors on terrestrial NPP variations. However, several limitations of the utilized approach should be recognized. First, the current version of the CASA model neglects the contributions of mineralization (Zhao and Li, 2017), ozone exposure (Ren et al., 2007) and land management practices (i.e. fertilization, irrigation and grazing) (Rost et al., 2009) to NPP variations, which limits its capacity of estimating the terrestrial NPP (Potter et al., 1999; Zhao et al., 2005). The use of a progress-based model can potentially solve this problem. Second, the obtained results were negatively affected by the mismatched spatial scales of the urban land (30 m) and NDVI (1 km) data as well as by the inadequate temporal coverage of the land cover data (2000–2010), which required the use of additional vegetation index and land cover data with higher resolutions and longer time spans to reduce the resulting uncertainties. Third, NPP changes are driven by multiple interacting factors; hence, additional studies must be performed to examine their individual contributions to terrestrial NPP variations (especially in the regions with dominant residual factors). Finally, the urban expansion speed for each year between 2000 and 2010 was assumed as a constant value, this assumption was not so robust since there exhibited great spatio-temporal variations of the urban sprawl speed in China. Using more land use data will be a nice try, which can improve the results' reliability greatly.

5. Conclusions

In this study, the effects of urbanization and climate change on NPP variations during 2000–2010 in China were determined on a macroscale. From the obtained results, the following conclusions were drawn. (I) The urban expansion during the study period resulted in NPP losses reaching 11.60×10^{-3} Pg C, which were widely observed in East China and the Northeast and North China plains, and were most severe in the highly urbanized regions. The urban expansion areas and average NPP values of the newly urbanized regions affected the magnitudes of NPP losses caused by urbanization. (II) Urban expansion strongly offset the NPP increases induced by climate change. The offsetting ratio calculated for China was 5.42%, and its exact magnitudes varied by province. (III) Urban expansion dominated the NPP variations in the regions with rapid urban expansion. Climate change drove the NPP variations over the arid and semi-arid ecosystems and Tibet Plateau, and contributed less to the NPP changes on the national scale as compared to the effect produced by residual factors, which were dominant over the central and southeastern regions of China.

Acknowledgments

This work was funded by the National Key R & D Program of China (Grant No. 2017YFA0604404), the Key National Natural Science Foundation of China (Grant No. 41531176), and the National Natural Science Foundation of China (Grant No. 41671398).

Appendix A. Supplementary data

Supplementary data to this article can be found online at https://doi.org/10.1016/j.jenvman.2019.03.071.

References

Chen, J., Chen, J., Liao, A., Cao, X., Chen, L., Chen, X., He, C., Han, G., Peng, S., Lu, M., Zhang, W., Tong, X., Mills, J., 2015. Global land cover mapping at 30m resolution: a POK-based operational approach. ISPRS J. Photogramm. 7–27. https://doi.org/10.1016/j.isprsjprs.2014.09.002.

Didan, K., 2015. MOD13A3 MODIS/Terra Vegetation Indices Monthly L3 Global 1km SIN Grid V006. [NDVI]. https://doi.org/10.5067/MODIS/MOD13A3.006.

FAO, IIASA, ISRIC, ISSCAS, JRC, 2012. Harmonized World Soil Database, Version 1.2.

Feng, X., Liu, G., Chen, J., Chen, M., Liu, J., Ju, W., Sun, R., Zhou, W., 2007. Net primary productivity of China's terrestrial ecosystems from a process model driven by remote sensing. J. Environ. Manage. 3, 563–573. https://doi.org/10.1016/j.jenvman.2006.09.021.

Finzi, A.C., Norby, R.J., Calfapietra, C., Gallet-Budynek, A., Gielen, B., Holmes, W.E., Hoosbeek, M.R., Iversen, C.M., Jackson, R.B., Kubiske, M.E., Ledford, J., Liberloo, M., Oren, R., Polle, A., Pritchard, S., Zak, D.R., Schlesinger, W.H., Ceulemans, R., 2007. Increases in nitrogen uptake rather than nitrogen-use efficiency support higher rates of temperate forest productivity under elevated CO2. Proc. Natl. Acad. Sci. USA 35, 14014–14019. https://doi.org/10.1073/pnas.0706518104.

Friedl, M., Sulla-Menashe, D., 2015. MCD12Q1 MODIS/Terra+Aqua Land Cover Type Yearly L3 Global 500m SIN Grid V006. https://doi.org/10.5067/MODIS/MCD12Q1.006.

Gao, Z., Liu, J., 2008a. Comparative study on net primary productivity of vegetation in China. Chinese Sci. Bull. 03, 317–326.

Gao, Z., Liu, J., 2008b. Simulation study of China's net primary production. Chinese Sci. Bull. 53, 434–443. https://doi.org/10.1007/s11434-008-0097-8.

Gao, Y., Yu, G., Zhang, L., Liu, M., Huang, M., Wang, Q., 2012. The changes of net primary productivity in Chinese terrestrial ecosystem: based on process and parameter models. Prog. Geogr. 109–117. https://doi.org/10.11820/dlkxjz.2012.01.014.

Gu, J., Li, X., Huang, C., 2012. Changes in Satellite-Derived Vegetation Growth Trend in China from 2002 to 2010. (Paper presented at the SPIE Remote Sensing).

Gu, F., Zhang, Y., Huang, M., Tao, B., Guo, R., Yan, C., 2017. Effects of climate warming on net primary productivity in China during 1961–2010. Ecol. Evol. 17, 6736–6746. https://doi.org/10.1002/ece3.3029.

Harris, I., Jones, P.D., Osborn, T.J., Lister, D.H., 2014. Updated high-resolution grids of monthly climatic observations – the CRU TS3.10 Dataset. Int. J. Climatol. 3, 623–642. https://doi.org/10.1002/joc.3711.

Imhoff, M.L., Bounoua, L., Defries, R., Lawrence, W.T., Stutzer, D., Tucker, C.J., Ricketts, T., 2004. The consequences of urban land transformation on net primary productivity in the United States. Remote Sens. Environ. 4, 434–443. https://doi.org/10.1016/j.rse.2003.10.015.

Jiang, C., Wu, Z., Cheng, J., Yu, Q., Rao, X., 2015. Impacts of urbanization on net primary productivity in the Pearl River Delta, China. Int. J. Plant Prod. 4, 581–598. https://doi.org/10.22069/ijpp.2015.2464.

Krausmann, F., Erb, K.-H., Gingrich, S., Haberl, H., Bondeau, A., Gaube, V., Lauk, C., Plutzar, C., Searchinger, T.D., 2013. Global human appropriation of net primary production doubled in the 20th century. Proc. Natl. Acad. Sci. USA. 25, 10324. https://doi.org/10.1073/pnas.1211349110.

Li, Q., Zhang, C., Shen, Y., Jia, W., Li, J., 2016a. Quantitative assessment of the relative roles of climate change and human activities in desertification processes on the Qinghai-Tibet Plateau based on net primary productivity. Catena 789–796. https://doi.org/10.1016/j.catena.2016.09.005.

Li, X., Yu, L., Liu, X., Gong, P., 2016b. Forecasting Global Urban Expansion and its Effect on Terrestrial Net Primary Productivity. (Paper presented at the EGU General Assembly Conference).

Li, X., Chen, G., Liu, X., Liang, X., Wang, S., Chen, Y., Pei, F., Xu, X., 2017. A new global land-use and land-cover change product at a 1-km resolution for 2010 to 2100 based on human–environment interactions. Ann. Am. Assoc. Geogr. 5, 1040–1059. https://doi.org/10.1080/24694452.2017.1303357.

Liang, W., Yang, Y., Fan, D., Guan, H., Zhang, T., Long, D., Zhou, Y., Bai, D., 2015. Analysis of spatial and temporal patterns of net primary production and their climate controls in China from 1982 to 2010. Agr. Forest Meteorol. 22–36. https://doi.org/10.1016/j.agrformet.2015.01.015.

Liu, J., Zhang, Q., Hu, Y., 2012a. Regional differences of China's urban expansion from late 20th to early 21st century based on remote sensing information. Chinese Geogr. Sci. 1, 1–14. https://doi.org/10.1007/s11769-012-0510-8.

Liu, Y., Ju, W., He, H., Wang, S., Sun, R., Zhang, Y., 2012b. Changes of net primary productivity in China during recent 11 years detected using an ecological model driven by MODIS data. Front. Earth Sci-PRC. 1, 112–127. https://doi.org/10.1007/s11707-012-0348-5.

Liu, X., Liang, X., Li, X., Xu, X., Ou, J., Chen, Y., Li, S., Wang, S., Pei, F., 2017. A future land use simulation model (FLUS) for simulating multiple land use scenarios by coupling human and natural effects. Landscape Urban Plan 94–116. https://doi.org/10.1016/j.landurbplan.2017.09.019.

Lu, C., Tian, H., Liu, M., Ren, W., Xu, X., Chen, G., Zhang, C., 2012. Effect of nitrogen deposition on China's terrestrial carbon uptake in the context of multifactor environmental changes. Ecol. Appl. 1, 53–75. https://doi.org/doi:10.1890/10-1685.1.

Mao, D., Luo, L., Wang, Z., Zhang, C., Ren, C., 2015. Variations in net primary productivity and its relationships with warming climate in the permafrost zone of the Tibetan Plateau. J. Geogr. Sci. 8, 967–977. https://doi.org/10.1007/s11442-015-1213-8.

Nemani, R.R., Keeling, C.D., Hashimoto, H., Jolly, W.M., Piper, S.C., Tucker, C.J., Myneni, R.B., Running, S.W., 2003. Climate-driven increases in global terrestrial net primary production from 1982 to 1999. Science 5625, 1560–1563. https://doi.org/10.1126/science.1082750.

Ouyang, Z., Zheng, H., Xiao, Y., Polasky, S., Liu, J., Xu, W., Wang, Q., Zhang, L., Xiao, Y., Rao, E., Jiang, L., Lu, F., Wang, X., Yang, G., Gong, S., Wu, B., Zeng, Y., Yang, W., Daily, G.C., 2016. Improvements in ecosystem services from investments in natural capital. Science 6292, 1455–1459. https://doi.org/10.1126/science.aaf2295.

Pei, F., Li, X., Liu, X., Lao, C., 2013a. Assessing the impacts of droughts on net primary productivity in China. J. Environ. Manage. 2, 362–371. https://doi.org/10.1016/j.agrformet.2012.12.003.

Pei, F., Li, X., Liu, X., Wang, S., He, Z., 2013b. Assessing the differences in net primary productivity between pre- and post-urban land development in China. Agr. Forest Meteorol 174–186. https://doi.org/10.1016/j.agrformet.2012.12.003.

Pei, F., Li, X., Liu, X., Lao, C., Xia, G., 2015. Exploring the response of net primary productivity variations to urban expansion and climate change: a scenario analysis for Guangdong Province in China. J. Environ. Manag. 92–102. https://doi.org/10.1016/

j.jenvman.2014.11.002.
Piao, S., Fang, J., Zhou, L., Zhu, B., Tan, K., Tao, S., 2005. Changes in vegetation net primary productivity from 1982 to 1999 in China. Global Biogeochem. Cy. 2. https://doi.org/10.1029/2004gb002274.
Potter, C.S., Randerson, J.T., Field, C.B., Matson, P.A., Vitousek, P.M., Mooney, H.A., Klooster, S.A., 1993. Terrestrial ecosystem production: a process model based on global satellite and surface data. Global Biogeochem. Cy. 4, 811–841. https://doi.org/10.1029/93GB02725.
Potter, C.S., Klooster, S., Brooks, V., 1999. Interannual variability in terrestrial net primary production: exploration of trends and controls on regional to global scales. Ecosystems 1, 36–48. https://doi.org/10.1007/s100219900056.
Potter, C.S., Klooster, S., Genovese, V., 2012. Net primary production of terrestrial ecosystems from 2000 to 2009. Clim. Change 2, 365–378. https://doi.org/10.1007/s10584-012-0460-2.
Ren, W., Tian, H., Liu, M., Zhang, C., Chen, G., Pan, S., Felzer, B., Xu, X., 2007. Effects of tropospheric ozone pollution on net primary productivity and carbon storage in terrestrial ecosystems of China. J. Geophys. Res. D22. https://doi.org/10.1029/2007jd008521.
Rost, S., Gerten, D., Hoff, H., Lucht, W., Falkenmark, M., 2009. Global potential to increase crop production through water management in rainfed agriculture. Environ. Res. Lett. 4, 044002. https://doi.org/10.1088/1748-9326/4/4/044002.
Roxburgh, S.H., Berry, S.L., Buckley, T.N., Barnes, B., Roderick, M.L., 2005. What is NPP? Inconsistent accounting of respiratory fluxes in the definition of net primary production. Funct. Ecol. 3, 378–382. https://doi.org/10.1111/j.1365-2435.2005.00983.x.
Running, S.W., Thornton, P.E., Nemani, R., Glassy, J.M., 2000. Global terrestrial gross and net primary productivity from the earth observing system. Methods Ecosyst. Sci. 44–57. https://doi.org/10.1007/978-1-4612-1224-9_4.
Shao, J., Zhou, X., Luo, Y., Zhang, G., Yan, W., Li, J., Li, B., Dan, L., Fisher, J.B., Gao, Z., He, Y., Huntzinger, D., Jain, A.K., Mao, J., Meng, J., Michalak, A.M., Parazoo, N.C., Peng, C., Poulter, B., Schwalm, C.R., Shi, X., Sun, R., Tao, F., Tian, H., Wei, Y., Zeng, N., Zhu, Q., Zhu, W., 2016. Uncertainty analysis of terrestrial net primary productivity and net biome productivity in China during 1901–2005. J. Geophys. Res.-Biogeo. 5, 1372–1393. https://doi.org/doi:10.1002/2015JG003062.
Sheffield, J., Goteti, G., Wood, E.F., 2006. Development of a 50-year high-resolution global dataset of meteorological forcings for land surface modeling. J. Climate 3088–3111. https://doi.org/10.1175/jcli3790.1.
Song, W., Deng, X., 2015. Effects of urbanization-induced cultivated land loss on ecosystem services in the north China plain. Energies 6, 5678. https://doi.org/10.3390/en8065678.
Song, Y., Ma, M., 2011. A statistical analysis of the relationship between climatic factors and the Normalized Difference Vegetation Index in China. Int. J. Remote Sens. 14, 3947–3965. https://doi.org/10.1080/01431161003801336.
Sun, R., Zhu, Q., 2001. Effect of climate change on terrestrial net primary productivity in China. J. Remote Sens.-Beijing 1, 61–62.
Sun, S., Song, Z., Wu, X., Wang, T., Wu, Y., Du, W., Che, T., Huang, C., Zhang, X., Ping, B., Lin, X., Li, P., Yang, Y., Chen, B., 2018. Spatio-temporal variations in water use efficiency and its drivers in China over the last three decades. Ecol. Indic 292–304. https://doi.org/10.1016/j.ecolind.2018.07.003.
Thomas, R.T., Prentice, I.C., Graven, H., Ciais, P., Fisher, J.B., Hayes, D.J., Huang, M., Huntzinger, D.N., Ito, A., Jain, A., Mao, J., Michalak, A.M., Peng, S., Poulter, B., Ricciuto, D.M., Shi, X., Schwalm, C., Tian, H., Zeng, N., 2016. Increased light-use efficiency in northern terrestrial ecosystems indicated by CO2 and greening observations. Geophys. Res. Lett. 21 (11) 339-311,349. https://doi.org/10.1002/2016GL070710.
Tian, G., Qiao, Z., 2014. Assessing the impact of the urbanization process on net primary productivity in China in 1989–2000. Environ. Pollut. 320–326. https://doi.org/10.1016/j.envpol.2013.09.012.
Tian, H., Melillo, J., Lu, C., Kicklighter, D., Liu, M., Ren, W., Xu, X., Chen, G., Zhang, C., Pan, S., Liu, J., Running, S., 2011. China's terrestrial carbon balance: contributions from multiple global change factors. Global Biogeochem. Cy. 1. https://doi.org/10.1029/2010gb003838.
Wang, J., 2004. Chinese Terrestrial Net Ecosystem Productive Model Applied Remote Sensing Data. Dissertation for Ph.D. Degree. Hangzhou-Zhejiang University (in Chinese).
Wang, H., Liu, G., Li, Z., Ye, X., Wang, M., Gong, L., 2016. Impacts of climate change on net primary productivity in arid and semiarid regions of China. Chinese Geogr. Sci. 1, 35–47. https://doi.org/10.1007/s11769-015-0762-1.
Wang, J., Dong, J., Yi, Y., Lu, G., Oyler, J., Smith, W.K., Zhao, M., Liu, J., Running, S., 2017. Decreasing net primary production due to drought and slight decreases in solar radiation in China from 2000 to 2012. J. Geophys. Res.-Biogeo. 1, 261–278. https://doi.org/doi:10.1002/2016JG003417.
Wen, Y., Liu, X., Pei, F., Li, X., Du, G., 2018. Non-uniform time-lag effects of terrestrial vegetation responses to asymmetric warming. Agr. Forest Meteorol. 130–143. https://doi.org/10.1016/j.agrformet.2018.01.016.
Wu, S., Zhou, S., Chen, D., Wei, Z., Liang, D., Li, X., 2014. Determining the contributions of urbanisation and climate change to NPP variations over the last decade in the Yangtze River Delta, China. Sci. Total Environ. 397–406. https://doi.org/10.1016/j.scitotenv.2013.10.128.
Wu, Y., Wu, Z., Yu, S., 2017. Quantitatively evaluating the impact of human activities on net primary productivity. Chinese J. Appl. Ecol. 8. https://doi.org/10.1007/s11356-018-1431-6.
Xiao, J., Zhou, Y., Zhang, L., 2015. Contributions of natural and human factors to increases in vegetation productivity in China. Ecosphere 11, art233. https://doi.org/10.1890/es14-00394.1.
Xu, G., Zhang, H., Chen, B., Zhang, H., Innes, J., Wang, G., Yan, J., Zheng, Y., Zhu, Z., Myneni, R., 2014. Changes in vegetation growth dynamics and relations with climate over China's landmass from 1982 to 2011. Remote Sens.(Basel) 4, 3263–3283. https://doi.org/10.3390/rs6043263.
Yan, H., Zhan, J., Wu, F., Yang, H., 2016. Effects of climate change and LUCC on terrestrial biomass in the lower Heihe river basin during 2001–2010. Energies 4, 260. https://doi.org/10.3390/en9040260.
Yan, H., Zhan, J., Yang, H., Liu, W., Li, W., 2018a. Wind erosion reduction by water diversion in the lower Heihe River Basin, Northwest China. Land Degr. Dev. 6, 1906–1914. https://doi.org/10.1002/ldr.2927.
Yan, Y., Liu, X., Wang, F., Li, X., Ou, J., Wen, Y., Liang, X., 2018b. Assessing the impacts of urban sprawl on net primary productivity using fusion of Landsat and MODIS data. Sci. Total Environ. 1417–1429. https://doi.org/10.1016/j.scitotenv.2017.09.139.
Yu, B., Chen, F., 2016. The global impact factors of net primary production in different land cover types from 2005 to 2011. SpringerPlus 1 1235-1235. https://doi.org/10.1186/s40064-016-2910-1.
Zhang, J., Yao, F., Zheng, L., Yang, L., 2007. Evaluation of grassland dynamics in the northern-Tibet Plateau of China using remote sensing and climate data. Sensors 12, 3312–3328. https://doi.org/10.3390/s7123312.
Zhang, C., Tian, H., Pan, S., Lockaby, G., Chappelka, A., 2014a. Multi-factor controls on terrestrial carbon dynamics in urbanised areas. Biogeosci. Discuss. 10, 17597–17631. https://doi.org/10.5194/bg-11-7107-2014.
Zhang, Y., Song, C., Zhang, K., Cheng, X., Band, L.E., Zhang, Q., 2014b. Effects of land use/land cover and climate changes on terrestrial net primary productivity in the Yangtze River Basin, China, from 2001 to 2010. J. Geophys. Res.-Biogeo. 6, 1092–1109. https://doi.org/10.1002/2014jg002616.
Zhao, N., Li, X., 2017. Effects of aspect–vegetation complex on soil nitrogen mineralization and microbial activity on the Tibetan Plateau. Catena 1–9. https://doi.org/10.1016/j.catena.2017.02.025.
Zhao, M., Running, S.W., 2010. Drought-induced reduction in global terrestrial net primary production from 2000 through 2009. Science 5994, 940–943. https://doi.org/10.1126/science.1192666.
Zhao, M., Heinsch, F.A., Nemani, R.R., Running, S.W., 2005. Improvements of the MODIS terrestrial gross and net primary production global data set. Remote Sens. Environ. 2, 164–176. https://doi.org/10.1016/j.rse.2004.12.011.
Zhu, W., Pan, Y., He, H., Yu, D., Hu, H., 2006. Simulation of maximum light use efficiency for some typical vegetation types in China. Chinese Sci. Bull. 4, 457–463. https://doi.org/10.1007/s11434-006-0457-1.
Zhu, W., Pan, Y., Yang, X., Song, G., 2007. Analyzing the impacts of climate change on terrestrial net primary productivity in China. Chinese Sci. Bull. 21, 2535–2541. https://doi.org/10.3321/j.issn:0023-074x.2007.21.012.
Zhu, Z., Piao, S., Myneni, R.B., Huang, M., Zeng, Z., Canadell, J.G., Ciais, P., Sitch, S., Friedlingstein, P., Arneth, A., Cao, C., Cheng, L., Kato, E., Koven, C., Li, Y., Lian, X., Liu, Y., Liu, R., Mao, J., Pan, Y., Peng, S., Peñuelas, J., Poulter, B., Pugh, T.A.M., Stocker, B.D., Viovy, N., Wang, X., Wang, Y., Xiao, Z., Yang, H., Zaehle, S., Zeng, N., 2016. Greening of the Earth and its drivers. Nat. Clim. Change 8, 791–795. https://doi.org/10.1038/nclimate3004.